PHYSICAL REVIEW B VOLUME 53, NUMBER 5 1 FEBRUARY 1996-I

Bipolaron anisotropic flat bands, Hall mobility edge, and metal-semiconductor duality of overdoped high-T_c oxides

A. S. Alexandrov
Department of Physics, Loughborough University of Technology, Loughborough LE11 3TU, United Kingdom and Interdisciplinary Research Centre in Superconductivity, University of Cambridge, Madingley Road, Cambridge CB3 0HE, United Kingdom

(Received 30 March 1995; revised manuscript received 1 September 1995)

Hole bipolaron band structure with two flat anisotropic bands is derived for oxide superconductors. Strong anisotropy leads to one-dimensional localization in a random field which explains the *metal-like* value of the Hall effect and the *semiconductorlike* doping dependence of resistivity of overdoped oxides. Doping dependence of T_c and $\lambda_H(0)$ as well as the low-temperature dependence of resistivity, of the Hall effect, $H_{c2}(T)$ and robust features of angle-resolved photoemission spectroscopy of several high-T_c copper oxides are explained.

I. INTRODUCTION

The ''parent'' Mott insulators suggest that high-T_c superconductors are in fact doped semiconductors. There is now a growing consensus that the dopant-induced charge carriers in high-T_c oxides exhibit a significant dressing due to spin,[1] charge,[2] and lattice[3] fluctuations. Studies of strongly correlated models like the Holstein t-J model show that the critical electron-phonon coupling strength for polaron formation is considerably reduced by an antiferromagnetic exchange interaction compared to that in the uncorrelated model.[4] There is also a growing experimental evidence that polarons and bipolarons are carriers in high-temperature superconductors. In particular, studies of photoinduced carriers in dielectric parent compounds like La_2CuO_4 and $YBa_2Cu_3O_6$ as well as the infrared conductivity of metallic compounds confirm the formation of self-localized polarons.[5,6] A direct evidence for small polarons in doped copper oxides has been provided by Calvani *et al.*[7] with infrared spectroscopy. An oxygen isotope effect on the Néel temperature has been found in La_2CuO_4 suggesting the oxygen-mass dependence of superexchange J due to the small polaron band narrowing.[8] The crucial role of apex oxygen ions in the polaron formation has been verified for La-Sr-Cu-O (LSCO). Assuming that the carriers in a doped Mott insulator are spin-lattice bipolarons moving in a random potential Mott and the author explained several unusual features of the low-energy kinetics and thermodynamics of *underdoped* copper oxides.[3]

On the other hand, it has been suggested that optimally doped and overdoped oxides are metals with a large Fermi surface as follows from angle-resolved photoemission spectroscopy (ARPES), the T^2 temperature dependence of resistivity, and from the small value of the Hall effect. A three-band model involving a strong oxygen-copper hybridization [Fig. 1(a)] has been studied by several authors as a relevant one. However, the recent progress in elucidating the normal state of the prototypical cuprate $La_{2-x}Sr_xCuO_4$,[9,10] and of overdoped $Tl_2Ba_2CuO_6$,[11] as well as the unusual $H_{c2}(T)$ of $Tl_2Ba_2CuO_6$ (Ref. 12) and $Bi_2Sr_2CuO_y$ (Ref. 13) led several authors to the conclusion that low-energy kinetics of *overdoped* oxides is inconsistent with the Fermi-liquid picture[14,11] and with the spin-charge separation picture.[9] In particular, semiconductorlike scaling with x of dc conductivity of $La_{2-x}Sr_xCuO_4$ for a wide temperature and doping region[10] and the *linear* low-temperature resistivity ρ as well as the *linear* Hall effect in overdoped $Tl_2Ba_2CuO_6$,[11] have been observed.

Sometimes it is argued that unusual features of overdoped high-T_c oxides can be understood as a result of a strong magnetic pair breaking if the spin-flip mean free path l_s is shorter than the coherence length ξ_0. However high-T_c oxides are at a ''clean'' limit, the mean free path l is at least 20 times larger than ξ_0.[12,11] This makes the magnetic pair breaking irrelevant for high-T_c because the strong inequality $l_s \ll l$ is unrealistic; normally $l_s \gg l$.

In this paper the oxygen hole energy dispersion is studied with the model electron-phonon interaction taking into account the self-trapping effect and the attraction between in-

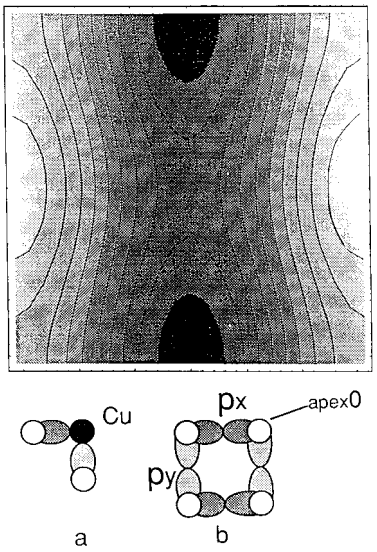

FIG. 1. Counterplot of the x bipolaron dispersion $E^x_{\mathbf{k}}$. Dark regions correspond to the bottom of the band. $E^y_{\mathbf{k}}$ energy surfaces are obtained by $\pi/2$ rotation. Three-band (t-J) model (a) and two-band apex bipolaron model (b).

plane and apex holes. The role of copper in electronic transport is significantly reduced by bipolaron formation. A simple two-band model is derived with a strong a-b anisotropy of two narrow bipolaron oxygen bands. The effective-mass anisotropy is 4 or larger. A random potential increases the anisotropy, so low-energy carriers are effectively localized in one direction for a wide range of doping. Then there is a "Hall mobility edge" E_{cH}. The states below E_{cH} contribute to the longitudinal conductivity rather than to the transverse one. A quantitative explanation for a high value of the Hall density in $La_{2-x}Sr_xCuO_4$ is proposed compatible with the x scaling of dc conductivity. The doping dependence of T_c and of λ_H both in underdoped and overdoped samples, the low-temperature dependence of ρ, R_H, and H_{c2} of overdoped $Tl_2Ba_2CuO_6$ and the robust features of ultrahigh energy resolution angle-resolved photoemission spectra[15,16] (ARPES) are explained with bipolarons.

II. TWO-BAND BIPOLARON MODEL

The hole in a square oxygen-copper lattice hops directly from one oxygen ion to its oxygen neighbor due to an overlap of p oxygen orbitals, Fig. 1(b), or via a second-order indirect transition involving d orbitals of copper, Fig. 1(a). While the direct tunneling is linear in the oxygen-oxygen hopping integral $T_{pp'}$, the indirect transition is of the second order in the oxygen-copper hopping T_{pd}. There is an assumption within the three-band model that the indirect hopping is more important because of a shorter copper-oxygen distance compared with an oxygen-oxygen one and of the relatively small size of the charge-transfer gap $E_g \simeq 1-2$ eV. A strong Fröhlich-type interaction modifies essentially the energy spectrum. To show this I consider the model Hamiltonian

$$H=\sum_{i,j} T_{ij}c_i^\dagger c_j+\sum_{\mathbf{q},j} \omega_{\mathbf{q}} n_j[u_j(\mathbf{q})d_{\mathbf{q}}+\text{H.c.}]+\sum_{\mathbf{q}} \omega_{\mathbf{q}} d_{\mathbf{q}}^\dagger d_{\mathbf{q}} + \frac{1}{2}\sum_{i,j} V_{ij}n_i n_j, \tag{1}$$

where T_{ij} determines the bare band structure in the site representation; c_i, c_j are hole annihilation operators for oxygen or copper sites i,j; $n_j=c_j^\dagger c_j$ is the number operator, V_{ij} is the direct Coulomb repulsion, which does not include the on-site term $i=j$ for parallel spins; $\omega_{\mathbf{q}}, d_{\mathbf{q}}$ are the phonon frequency and annihilation operator, respectively. The electron-phonon coupling in the site representation for electrons is given by

$$u_j(\mathbf{q})=\frac{1}{\sqrt{2N}}\gamma(\mathbf{q})e^{i\mathbf{q}\cdot\mathbf{m}_j}, \tag{2}$$

where N is the number of cells in the normalized volume $N\Omega$, $\mathbf{m}_j$ is the lattice vector. Oxides are strongly polarizable materials, so coupling with optical phonons dominates in the electron-phonon interaction

$$\gamma(\mathbf{q})=-\frac{i\sqrt{8\pi\alpha}}{\sqrt{\Omega}(2m\omega)^{1/4}q} \tag{3}$$

with the dimensionless coupling constant $\alpha=e^2(\epsilon_\infty^{-1}-\epsilon_0^{-1})\sqrt{m/2\omega}$, introduced by Fröhlich,[17] and the momentum-independent optical phonon frequency $\omega_{\mathbf{q}}=\omega$. The lattice polarization is coupled with the electron density, therefore the interaction is diagonal in the site representation and the coupling constant does not depend on the particular orbital. In doped oxides optical phonons are partially screened. Then molecular $\omega_{\mathbf{q}}=\omega_0$ and acoustical $\omega_{\mathbf{q}}=sq$ phonons contribute also to the interaction with the coupling constants $\gamma\equiv\gamma_0$ and $\gamma\sim 1/\sqrt{q}$, respectively. The canonical displacement transformation $S=\exp\{\Sigma_{\mathbf{q},j}n_j[u_j(\mathbf{q})d_{\mathbf{q}}-\text{H.c.}]\}$ eliminates an essential part of the electron-phonon interaction. The transformed Hamiltonian is given by[3]

$$\tilde{H}=SHS^{-1}=(T_p-E_p)\sum_{i(p)} n_{i(p)}+(T_d-E_d)\sum_{i(d)} n_{i(d)} + \sum_{i\neq j} \hat{\sigma}_{ij}c_i^\dagger c_j+\sum_{\mathbf{q}} \omega_{\mathbf{q}} d_{\mathbf{q}}^\dagger d_{\mathbf{q}} - \frac{1}{2}\sum_{\mathbf{q},i,j}[2\omega_{\mathbf{q}}u_i(\mathbf{q})u_j^*(\mathbf{q})-V_{ij}]n_i n_j. \tag{4}$$

The first oxygen (p) and the second copper (d) diagonal terms include the polaronic level shift, which is the same for oxygen and copper ions

$$E_p=E_d=\sum_{\mathbf{q}} |u_j(\mathbf{q})|^2\omega_{\mathbf{q}}. \tag{5}$$

The transformed hopping term involves phonon operators

$$\hat{\sigma}_{ij}=T_{ij}\exp\left(\sum_{\mathbf{q}} u_i^*(\mathbf{q})d_{\mathbf{q}}^\dagger-\text{H.c.}\right)\exp\left(\sum_{\mathbf{q}} u_j(\mathbf{q})d_{\mathbf{q}}-\text{H.c.}\right). \tag{6}$$

There are two major effects of the electron-phonon interaction. One is the band narrowing due to a phonon cloud around the hole. In case of $E_g \gg \omega$ the bandwidth reduction factor is the same for the direct $t_{pp'}$ and the second-order via copper $t_{pp'}^{(2)}$ oxygen-oxygen transfer integrals (see the Appendix)

$$t_{pp'}\equiv\langle 0|\hat{\sigma}_{pp'}|0\rangle=T_{pp'}e^{-g_{pp'}^2}, \tag{7}$$

$$t_{pp'}^{(2)}\equiv\sum_\nu \frac{\langle 0|\hat{\sigma}_{pd}|\nu\rangle\langle\nu|\tilde{\sigma}_{dp'}|0\rangle}{E_0-E_\nu}\simeq\frac{T_{pd}^2}{E_g}e^{-g_{pp'}^2}, \tag{8}$$

where $|\nu\rangle$, E_ν are eigenstates and eigenvalues of the transformed Hamiltonian, Eq. (4) without the hopping term, $|0\rangle$ the phonon vacuum, and the reduction factor is

$$g_{pp'}^2=\frac{1}{2N}\sum_{\mathbf{q}} |\gamma(\mathbf{q})|^2\{1-\cos[\mathbf{q}\cdot(\mathbf{m}_p-\mathbf{m}_{p'})]\}. \tag{9}$$

Because the nearest-neighbor oxygen-oxygen distance in copper oxides is less than the lattice constant the calculation yields a remarkably lower value of $g_{pp'}^2\simeq 0.2E_p/\omega$ than one can expect with a naive estimation ($\simeq E_p/\omega$) (see the Appendix).

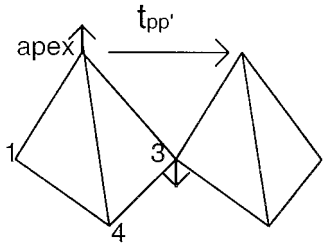

FIG. 2. Apex bipolaron tunneling between two copper polyhedra.

The other effect of the electron-phonon coupling is the attraction between two polarons given by the last term in Eq. (4). For the Fröhlich interaction the polaron level shift determined by Eq. (5) is

$$E_p \simeq \frac{q_D e^2}{\pi}(\epsilon_\infty^{-1} - \epsilon_0^{-1}), \tag{10}$$

where $q_d = (6\pi^2/\Omega)^{1/3}$ is the Debye momentum. With the static and high-frequency dielectric constants $\epsilon_0 \gg \epsilon_\infty \simeq 5$ and $q_D \simeq 0.7$ Å^{-1} one estimates $E_p \simeq 0.64$ eV and with $\omega = 0.06$ eV, $g^2_{pp'} \simeq 2$. As a result a large attraction between two polarons of the order of $2E_p \simeq 1$ eV is possible accompanied by the band mass enhancement less than one order of magnitude. This is in contrast with some assessments of the bipolaronic mechanism of high-T_c superconductivity based on the incorrect estimation of the effective mass.

The polaron-polaron interaction is the sum of two large contributions of the opposite sign, last term in Eq. (4), which generally are large compared with the reduced polaron bandwidth. This is just the opposite regime to that of the BCS superconductor where the Fermi energy is the largest. In that case one can expect real-space bipolarons. Different types of bipolarons in La_2CuO_4 were investigated by Zhang and Catlow[18] with computer simulation techniques based on the minimization of the ground-state energy E_0 of the Hamiltonian Eq. (4) without the hopping term. The intersite pairing of the in-plane oxygen hole polaron with the *apex* one was found energetically favorable with the binding energy $\Delta = 0.119$ eV. Obviously this apex bipolaron can tunnel from one cell to another via a direct single polaron hopping from one apex oxygen to its apex neighbor, Fig. 2. The *bipolaron* hopping integral t is obtained by projecting the Hamiltonian, Eq. (4) onto the reduced Hilbert space containing only empty or doubly occupied elementary cells. The wave function of the apex bipolaron localized, say in the cell **m** is written as

$$|\mathbf{m}\rangle = \sum_{i=1}^{4} A_i c_i^\dagger c_{\text{apex}}^\dagger |0\rangle, \tag{11}$$

where i denotes the $p_{x,y}$ orbitals and spins of the four plane oxygen ions in the cell **m**, Fig. 2 and $c^\dagger_{\text{apex}}$ is the creation operator for the hole on one of the three *apex* oxygen orbitals with the spin, which is same or opposite to the spin of the plane hole, depending on the total spin of the bipolaron. The probability amplitudes A_i are normalized by the condition $|A_i| = 1/2$ because only four plane orbitals p_{x1}, p_{y2}, p_{x3}, and p_{y4} are relevant within the three-band model. The matrix element of the Hamiltonian Eq. (4) of the first order with respect to the transfer integral responsible for the bipolaron tunneling to the nearest-neighbor cell $\mathbf{m}+\mathbf{a}$ is

$$t = \langle \mathbf{m}|\tilde{H}|\mathbf{m}+\mathbf{a}\rangle = \frac{1}{4} T^{\text{apex}}_{pp'} e^{-g^2}, \tag{12}$$

where $T^{\text{apex}}_{pp'}$ is the single hole hopping between two apex ions, and

$$g^2 = \frac{1}{2N}\sum_{\mathbf{q}} |\gamma(\mathbf{q})|^2 [1 - \cos(q_x a)] \tag{13}$$

is the polaron narrowing factor. Here a is the in-plane lattice constant, which is also the nearest-neighbor apex-apex distance. As a result the hole bipolaron energy spectrum in a tight-binding approximation consists of two bands $E^{x,y}$ formed by the overlap of p_x and p_y *apex polaron* orbitals, respectively, Fig. 1(b):

$$E^x_{\mathbf{k}} = -t\,\cos(k_x) + t'\cos(k_y), \tag{14}$$

$$E^y_{\mathbf{k}} = t'\,\cos(k_x) - t\,\cos(k_y), \tag{15}$$

where the in-plane lattice constant is taken to be $a = 1$, t is the renormalized hopping integral, Eq. (12) between p orbitals of the same symmetry elongated in the direction of the hopping $(pp\sigma)$, and t' is the renormalized hopping integral in the perpendicular direction $(pp\pi)$.[19] Their ratio $t/t' = T^{\text{apex}}_{pp'}/T'^{\text{apex}}_{pp'} = 4$ as follows from the tables of hopping integrals in solids.[20] Two different bands are not mixed because $T^{\text{apex}}_{p_x,p'_y} = 0$ for the nearest neighbors. The random potential does not mix them either if it varies smoothly on the lattice scale. Consequently, one can distinguish x and y bipolarons with a lighter effective mass in the x or y direction, respectively. The apex z bipolaron, if formed is ca. four times less mobile than the x and y bipolarons. The bipolaron bandwidth is of the same order as the polaron one, which is a specific feature of the intersite bipolarons.

The polaronic features of the energy spectrum and bipolaron formation are in line with the extremely flat *anisotropic* bands measured recently with ARPES (Refs. 16 and 15) in several copper high-T_c oxides which display at least an order of magnitude less dispersion than the first-principles bandstructure methodology can provide.[16] I believe that this flatness is due to the polaron narrowing of the band, Eq. (12) and the anisotropy is due to the remarkable difference of p_x overlaps in x and y direction, respectively. If bipolarons are formed the spectral weight is shifted down by half of the bipolaron binding energy with respect to the chemical potential. This could provide an explanation why the flat band observed with ARPES in $YBa_2Cu_4O_8$ does not cross the Fermi level. It lies approximately 20 meV below the chemical potential[16] which means that the bipolaron binding energy is about $\Delta \simeq 40$ meV in this material. The ''static'' calculations by Zhang and Catlow[18] of the bipolaron binding energy depends on details of the perovskite crystal structures. In their modeling of small bipolarons in doped high-T_c La_2CuO_4 they treated holes as Cu^{3+} or O^- species placed in the dielectric matrix with the CuO_6 unit, Fig. 2. The energy of a region of the crystal surrounding the hole or the hole pair is then minimized with respect to the coordinates of the

ions within the region containing ~200–300 ions. The response of the more distant regions of the crystal is calculated using approximate procedures based on continuum model employing the relative permittivity of the material. With a proper choice of the interatomic potentials one can find the binding energy of the small bipolaron of different geometry with the accuracy within 0.01 eV. The pairing was studied for a variety of separations in three types of possible bipolaron (Cu^{3+}-Cu^{3+}, Cu^{3+}-O^-, and O^--O^- pairs). Intercopper and copper-oxygen intersite bipolarons are unstable both for interlayer and intralayer pairing, where the binding energy is negative for all separations studied. However, three stable O^--O^- configurations were found. For in-plane configuration the bipolaron is bound by ~0.06 eV, whereas apex bipolaron configuration is bound by ~0.12 eV. These two bound oxygen pairs are situated at the nearest-neighbor sites ($d=2.66$ Å) and next-nearest-neighbor sites ($d=3.11$ Å). There is also a slightly bound bipolaron with a binding energy of 0.001 eV at $d=3.58$ Å. When d is larger than 3.81 Å all the configurations are energetically unfavorable. Consequently, the binding energy of small bipolarons is strongly related not only to the distance of the pair but also to the detailed geometry of the site where the polaron is situated and to the dielectric properties of the matrix. It is not surprising that the bipolaron binding energy is not universal among different copper oxides.

III. THE HALL CONSTANT

It is well known that the effective-mass anisotropy of energy ellipsoids in a square (or cubic) lattice diminishes the value of the Hall constant as in Si or Ge. In the presence of disorder an x bipolaron can be localized in the y direction tunneling practically freely along x and a y bipolaron can be localized in the x direction remaining free along y.[21] That gives a very low metalliclike R_H which presumably is due to bipolarons with the energy above the *Hall mobility* edge, $E>E_{cH}$. At the same time the dc conductivity remains proportional to the number of bipolarons above the mobility edge, which lies below, $E_c<E_{cH}$. To support this conclusion quantitatively one can adopt the effective-mass approximation for a large part of the Brillouin zone near $(0,\pi)$ for the x and $(\pi,0)$ for the y bipolaron, Fig. 1,

$$E_{\mathbf{k}}^{x,y}=\frac{k_x^2}{2m_{x,y}}+\frac{k_y^2}{2m_{y,x}} \tag{16}$$

with $k_{x,y}$ taken relative to the band bottom positions and $m_x=1/t$, $m_y=4m_x$. The Boltzmann equation in the relaxation time approximation yields

$$R_H\sim\frac{\Sigma_{\mathbf{k},n=x,y}f'(E_{\mathbf{k}}^n)[(\partial^2E_{\mathbf{k}}^n/\partial k_x^2)(\partial E_{\mathbf{k}}^n/\partial k_y)^2-(\partial E_{\mathbf{k}}^n/\partial k_y)(\partial E_{\mathbf{k}}^n/\partial k_x)(\partial^2E_{\mathbf{k}}^n/\partial k_y\partial k_x)]}{[\Sigma_{\mathbf{k},n}f'(E_{\mathbf{k}}^n)(\partial E_{\mathbf{k}}^n/\partial k_x)^2]^2}, \tag{17}$$

where $f'(E_{\mathbf{k}}^n)$ is the derivative of the distribution function. Counting bipolarons (n_0), with the energy above E_{cH} in the numerator and above E_c in the denominator of Eq. (17) one obtains

$$2eR_H=\frac{4m_xm_yn_0}{[(m_x+m_y)n_0+m_yn_1]^2}, \tag{18}$$

where $n_0=x/2-n_L$ is the number of bipolarons with the energy above E_{cH}, which are free in both directions; n_L is the number of bipolarons localized *at least* in one direction, and n_1 is the number of bipolarons localized *only* in one direction. The number of bipolarons per cell localized at least in one direction is proportional to the number of random potential wells with the depth U larger than t'

$$n_L=B\int_{-\infty}^{-t'}\exp(-U^2/\gamma^2)dU. \tag{19}$$

The coefficient B is determined by the condition that all states of the Brillouin zone should be localized ($n_L=1$) if the random potential is very large, $\gamma\gg t'$. The average depth γ of random wells is proportional to the relative fluctuation of the dopant density, which is the square root of the mean density x (Ref. 22)

$$\gamma=\gamma_0\sqrt{x}. \tag{20}$$

Here γ_0 is the characteristic binding energy independent of the dopant density. That yields $B=2/\gamma\sqrt{\pi}$ and

$$n_0=x/2+\mathrm{erf}(\kappa/\sqrt{x})-1 \tag{21}$$

with $\kappa=t'/\gamma_0$. The number of bipolarons, n_0+n_1, above the mobility edge E_c contributing to the *longitudinal* conductivity remains practically equal to the chemical density $x/2$ in a wide range of κ which can be verified with Eq. (19) replacing t' for $t=4t'$. As a result, the Hall density $n_H=1/2eR_H$ to the chemical density ratio is given by

$$\frac{n_H}{x/2}=\frac{[5x+2\,\mathrm{erf}(\kappa/\sqrt{x})-2]^2}{16x[x+2\,\mathrm{erf}(\kappa/\sqrt{x})-2]} \tag{22}$$

with $\mathrm{erf}(z)=(2/\sqrt{\pi})\int_0^z\exp(-\xi^2)d\xi$. The agreement with experiment is almost perfect for $\kappa=0.57$, Fig. 3. Due to the mass anisotropy the low-temperature physical density n_H remains ~1.6 times larger than the chemical $x/2$ even for low doping when $n_L\ll x/2$. The dc conductivity scales with x in overdoped samples as observed[10] because $n_0+n_1\simeq x/2$ for all x. On the contrary, the density n_0 of carriers extended in both directions falls rapidly in overdoped samples, Fig. 3 (inset), due to increasing random potential fluctuations, proportional to $\sqrt{x}$. The mass anisotropy of the order of 4 can be seen commonly in doped semiconductors. However the anisotropy increases rapidly in overdoped samples. In fact, the

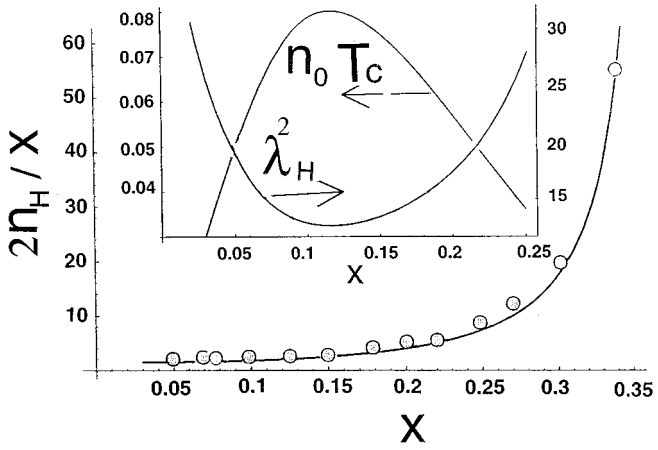

FIG. 3. The ratio of the Hall $n_H = 1/2eR_H$ to chemical $x/2$ densities in $La_{2-x}Sr_xCuO_4$ as a function of doping compared with experiment (Ref. 9) at 40 K. The size of the experimental circles includes an error bar due to temperature dependence of R_H below 50 K and the uncertainty in the oxygen content. Theoretical dependence of the density of extended bosons n_0, of T_c and of the penetration depth (in relative units) on doping (inset).

Hall to chemical density ratio, Fig. 3 is a measure of this anisotropy. At temperatures compared or higher than the bipolaron binding energy bipolarons coexist with unbound thermally excited polarons, which contribute also to the transport. In-plane polaronic bands are not so anisotropic as the apex bipolaron ones. That can explain why the Hall constant in LSCO depends less on doping at high temperatures compared with the low-temperature values.

IV. BIPOLARONS AND CRITICAL PARAMETERS OF HIGH-T_c COPPER OXIDES

The coherence volume determined with the heat-capacity measurements near T_c in many copper oxides is comparable or even less than the unit-cell volume.[23] That favors a charged $2e$ Bose liquid of small bipolarons as a plausible microscopic model of the superconducting state.[3]

The critical temperature of the superfluid phase transition in $2+\epsilon$ dimensions is proportional and the London penetration depth squared is inversely proportional to the density n_0 of delocalized bosons. Therefore

$$T_c \sim x + 2\ \mathrm{erf}(\kappa/\sqrt{x}) - 2 \tag{23}$$

and

$$\lambda_H^2(0) \sim \frac{1}{x + 2\ \mathrm{erf}(\kappa/\sqrt{x}) - 2}. \tag{24}$$

With Eqs. (23) and (24) one can easily explain the doping dependence of $T_c(x)$ in superconducting oxides as well as the so-called "Uemura" plot $T_c \sim 1/\lambda_H^2$ verified experimentally in underdoped and overdoped samples, Fig. 3 (inset).

As we have shown earlier[24] the density of delocalized bosons depends on temperature, increasing linearly for $T \ll \gamma$ in a "single-well–single-particle" approximation, $n_0(T) = n_0(0) + Tn_L \ln 2/\gamma$. That explains a linear increase of R_H with increasing temperature observed by Mackenzie *et al.*[11] in overdoped $Tl_2Ba_2CuO_6$ starting from the mK scale up to $\sim$30 K as follows from Eq. (18). The linear temperature dependence of resistivity at low temperatures[11] is explained by the fact that the number of unoccupied potential wells is proportional to temperature[24] as the number of extended bosons. Less screened they provide a strong temperature-dependent *elastic* scattering of bipolarons. With increasing temperature the boson-boson scattering dominates and the resistivity becomes proportional to T^2 as observed in overdoped oxides.

One can also describe the unusual temperature dependence of H_{c2} of a "low T_c" overdoped $Tl_2Ba_2CuO_{6+\delta}$,[12] as the critical field H^* of the Bose-Einstein condensation of charged bosons. Starting with the linearized stationary equation for the macroscopic condensate wave function $\psi_0(\mathbf{r})$

$$\left(-\frac{1}{2m}[\nabla - 2ie\mathbf{A}(\mathbf{r})]^2 + U_{im}(\mathbf{r}) \right) \psi_0(\mathbf{r}) = \mu \psi_0(\mathbf{r}), \tag{25}$$

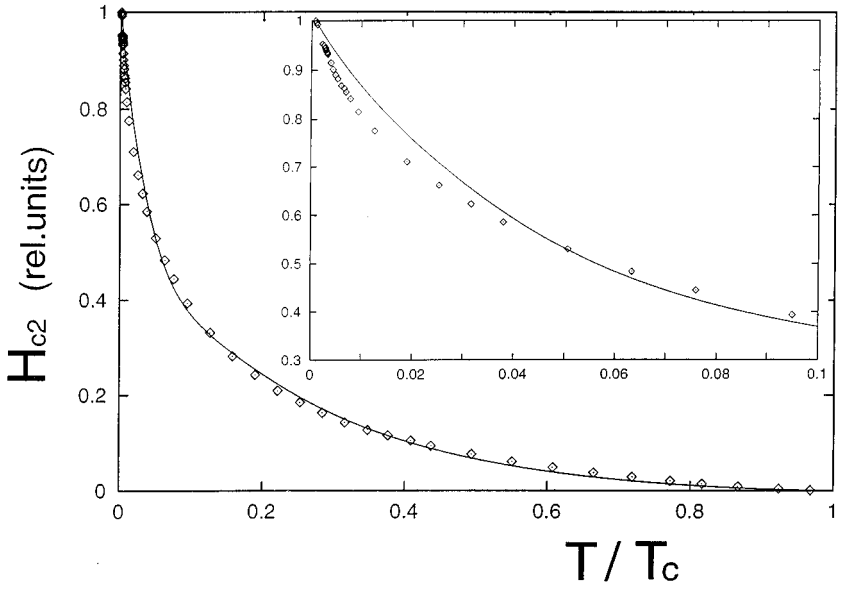

FIG. 4. Upper critical field of doped $Tl_2Ba_2CuO_{6+\delta}$ (Ref. 12) (points) compared with the critical field of the Bose-Einstein condensation, Eq. (26) from 15 mK up to $T_c \simeq 20$ K; inset represents the low-temperature part from 15 mK up to $\simeq 2$ K.

where $\mathbf{A}(\mathbf{r})$, $U_{im}(\mathbf{r})$, and μ are the vector, random, and chemical potentials, respectively, one arrives at[25]

$$H^*(T)=\text{const}\left(\frac{1-2n_L(t)/x}{t[1-2n_L(1)/x]}-\sqrt{t}\right)^{3/2}. \tag{26}$$

Here $t=T/T_c$, where T_c is the *experimental* critical temperature, x is the chemical *polaron* density determined in $Tl_2Ba_2CuO_{6+\delta}$ by the excess oxygen content δ, $x=2\delta$, and $n_L(t)$ is the number of localized bipolarons below E_{cH}. From Fig. 3 (inset) $x/2-n_L$ is very small in strongly overdoped samples. In fact, at zero temperature the condition $2n_L(0)/x=1$ is satisfied because each bipolaron is localized on the excess oxygen ion. In the ''single-well–single-particle'' approximation the number of localized bipolarons is determined by[24]

$$n_L(t)=\int_{-\infty}^{0} d\epsilon \frac{N_L(\epsilon)}{\exp(\epsilon/T)+1}, \tag{27}$$

where $N_L(\epsilon)$ is the density of localized states. The positive curvature of $H^*(T)$ on the temperature scale of the order of T_c does not depend on the particular shape of $N_L(\epsilon)$. However, at mK temperatures shallow potential wells are important. Therefore the low-temperature behavior of $H^*(T)$ is sensitive to the shape of $N_L(\epsilon)$ just below the mobility edge. One can model

$$N_L(\epsilon)=0.5n_L(0)\left[\frac{e^{\epsilon/\gamma}}{\gamma}+\delta(\epsilon-E_0)\right], \tag{28}$$

to imitate both the discrete levels with the energy E_0 and the exponential shallow tail due to the randomness of the impurity potential. Then one can quantitatively describe the experimental $H_{c2}(T)$ with Eq. (26) and $\gamma/T_c=0.13$ and $E_0/T_c=0.3$ for three decades of temperature, Fig. 4. This equation was also applied by Osofsky *et al.*[13] to describe the $H_{c2}(T)$ of $Bi_2Sr_2CuO_y$ with an excellent agreement for the critical temperature.[26]

V. CONCLUSIONS

In summary, the oxygen hole bipolaron bands of high-T_c oxides are derived manifesting a remarkable flatness and effective-mass anisotropy. The metallic value of the Hall effect and the semiconducting scaling of dc conductivity in overdoped high-T_c oxides are explained taking into account the Anderson localization of bipolarons. The doping dependence of the critical temperature and of the London penetration depth, the low-temperature dependences of resistivity, of the Hall ''constant'' and of the upper critical field as well as the robust features of ARPES are described.

The proposed two-band oxygen bipolaron model favors the spin-polaron formation as suggested by Mott for high-T_c copper oxides.[27] One conclusion is that copper electrons remain localized even in overdoped oxides because of the large Hubbard U on copper and the local lattice deformation, which prevents their hopping. Therefore the role of copper in electronic transport is significantly reduced. If so, one can envisage oxygen holes as heavy spin-lattice polarons surrounded by lattice and *copper* spin-polarized regions. Then both underdoped and overdoped high-T_c oxides are doped semiconductors with oxygen (bi)polarons as carriers partly localized by disorder. Another conclusion is that an estimation of the small (bi)polaron mass with the dispersionless Holstein model leads to an erroneous conclusion that small bipolarons are immobile. Taking into account the dispersion of the electron-phonon coupling constant and the perovskite crystal structure one obtains significantly less mass enhancement compared with this estimation and at the same time the polaron binding energy sufficient to overcome the intersite direct Coulomb repulsion.

This work is motivated by Mott's idea[27] that the localization of carriers in a random potential is crucial to our understanding of low-energy kinetics of high-T_c oxides which is receiving now an overwhelming experimental support.[3]

ACKNOWLEDGMENTS

The author is grateful to Sir Nevill Mott, Y. Liang, J. Wheatley, A. Bratkovsky, N. Hussey, V. Kabanov, and P. Kornilovich for valuable discussions. Victor Kabanov's help in numerical calculations and enlightening comments by Andy Mackenzie on the properties of overdoped materials are highly appreciated.

APPENDIX

Here the first- [Eqs. (7) and (12)] and the second-order [Eq. (8)] phonon averages and the reduction factors are calculated using the standard technique (see Ref. 3 and references therein). The direct hopping is given by

$$t_{pp'}=T_{pp'}\langle 0|\exp\left(\sum_{\mathbf{q}} u_p^*(\mathbf{q})d_{\mathbf{q}}^\dagger-\text{H.c.}\right)$$
$$\times\exp\left(\sum_{\mathbf{q}} u_{p'}(\mathbf{q})d_{\mathbf{q}}-\text{H.c.}\right)|0\rangle. \tag{A1}$$

With the help of $e^{A+B}=e^Ae^Be^{-[AB]/2}$ for any operators A, B with a c-number commutator one obtains

$$t_{pp'}=T_{pp'}e^{-g^2_{pp'}}\langle 0|\exp\left(\sum_{\mathbf{q}} u_p^*(\mathbf{q})d_{\mathbf{q}}^\dagger\right)$$
$$\times\exp\left(-\sum_{\mathbf{q}} u_{p'}(\mathbf{q})d_{\mathbf{q}}^\dagger\right)|0\rangle, \tag{A2}$$

where

$$g^2_{ij}=\frac{1}{2}\sum_{\mathbf{q}}\left[|u_i(\mathbf{q})|^2+|u_j(\mathbf{q})|^2-2u_i^*(\mathbf{q})u_j(\mathbf{q})\right]. \tag{A3}$$

The bracket in Eq. (A2) is equal unity. Then Eq. (9) follows from Eqs. (A2) and (A3) using the definition of $u_j(\mathbf{q})$, Eq. (2).

Taking into account that $E_\nu-E_0=E_g+\Sigma_{\mathbf{q}}\omega_{\mathbf{q}}n_{\mathbf{q}}$, the second-order indirect hopping Eq. (8) is written as

$$t^{(2)}_{pp'}=i\int_0^\infty dt\ e^{-iE_g t}\langle 0|\hat{\sigma}_{pd}(t)\hat{\sigma}_{dp'}|0\rangle, \tag{A4}$$

where

$$\hat{\sigma}_{pd}(t)=T_{pd}\ \exp\left(\sum_{\mathbf{q}}\ u^*_p(\mathbf{q},t)d^\dagger_{\mathbf{q}}-\text{H.c.}\right)$$

$$\times\exp\left(\sum_{\mathbf{q}}\ u_d(\mathbf{q},t)d_{\mathbf{q}}-\text{H.c.}\right). \tag{A5}$$

Here $u_j(\mathbf{q},t)\equiv u_j(\mathbf{q})\exp(i\omega_{\mathbf{q}}t)$ and $n_{\mathbf{q}}=0,1,2,...$ the phonon occupation numbers. Calculating the bracket in Eq. (A4) one obtains

$$\langle\ldots\rangle=e^{-g^2_{pd}}e^{-g^2_{dp'}}\ \exp\left(-\sum_{\mathbf{q}}\ [u_p(\mathbf{q})-u_d(\mathbf{q})]\right.$$

$$\left.\times[u^*_d(\mathbf{q})-u^*_{p'}(\mathbf{q})]e^{-i\omega_{\mathbf{q}}t}\right). \tag{A6}$$

If $\omega_{\mathbf{q}}$ is $\mathbf{q}$ independent the integral in Eq. (A4) is calculated by the expansion of the exponent in Eq. (A6):

$$t^{(2)}_{pp'}=\frac{T^2_{pd}}{E_g}e^{-g^2_{pd}}e^{-g^2_{dp'}}$$

$$\times\sum_{k=0}^{\infty}\frac{(-1)^k(\Sigma_{\mathbf{q}}[u_p(\mathbf{q})-u_d(\mathbf{q})][u^*_d(\mathbf{q})-u^*_{p'}(\mathbf{q})])^k}{k!(1+k\omega/E_g)}. \tag{A7}$$

Equation (8) is obtained from Eq. (A7) in the limit $E_g\gg\omega$.

Substitution of Eq. (3) into Eqs. (9) and (13) yields

$$g^2_{pp'},g^2=\frac{E_p}{\omega}\left(1-\frac{Si(q_d m)}{q_d m}\right), \tag{A8}$$

if the Debye approximation for the Brillouin zone is applied. Here $Si(x)=\int_0^x \sin(t)dt/t$, $m=a/\sqrt{2}$, and $m=a$ for the in-plane $g^2_{pp'}$ and for the apex reduction factor g^2, respectively. For LSCO with $q_d\simeq 0.7$ Å^{-1} and $a\simeq 3.8$ Å one obtains $g^2_{pp'}\simeq 0.2E_p/\omega$ and $g^2\simeq 0.3E_p/\omega$, where E_p is given by Eq. (10).

[1] For a review, see, E. Dagotto, Rev. Mod. Phys. **66**, 763 (1994).
[2] J. Lorenzana and L. Yu, Phys. Rev. B **43**, 11 474 (1991), and references therein.
[3] A. S. Alexandrov and N. F. Mott, Rep. Prog. Phys. **57**, 1197 (1994); *High Temperature Superconductors and Other Superfluids* (Taylor and Francis, London, 1994).
[4] H. Fehske *et al.*, Phys. Rev. B **51**, 16 582 (1995).
[5] D. Mihailovic *et al.*, Phys. Rev. B **42**, 7989 (1990).
[6] C. Taliani *et al.*, in *Electronic Properties of HT$_c$SC and Related Compounds*, edited by H. Kuzmany, M. Mehring, and J. Fink, Springer Series in Solid State Science (Springer-Verlag, Berlin, 1990), Vol. 99, p. 280.
[7] P. Calvani *et al.*, Solid State Commun. **91**, 113 (1994).
[8] G. Zhao, K. K. Singh, and D. E. Morris, Phys. Rev. B **50**, 4112 (1994).
[9] H. Y. Hwang *et al.*, Phys. Rev. Lett. **72**, 2636 (1994).
[10] B. Batlogg *et al.*, Physica C (Amsterdam) **235-240**, 130 (1994).
[11] A. P. Mackenzie *et al.* (unpublished).
[12] A. P. Mackenzie *et al.*, Phys. Rev. Lett. **71**, 1238 (1993).
[13] M. S. Osofsky *et al.*, Phys. Rev. Lett. **71**, 2315 (1993).
[14] R. G. Dias and J. M. Wheatley, Phys. Rev. B **50**, 13 887 (1994).
[15] D. M. King *et al.*, Phys. Rev. Lett. **73**, 3298 (1994).
[16] K. Gofron *et al.*, Phys. Rev. Lett. **73**, 3302 (1994).
[17] H. Fröhlich, in *Polarons and Excitons*, edited by C. G. Kuper and G. D. Whitfield (Oliver and Boyd, Edinburgh, 1963), p. 7.
[18] X. Zhang and C. R. A. Catlow, J. Mater. Chem. **1**, 233 (1991).
[19] A. S. Alexandrov and P. E. Kornilovitch (unpublished).
[20] W. A. Harrison, *Electronic Structure and the Properties of Solids* (Dover, New York, 1989), p. 552.
[21] Strictly speaking a one-dimensional localization is possible only for some exotic potentials. Here localization means an increase of the mass anisotropy due to disorder.
[22] L. D. Landau and E. M. Lifshitz, *Statistical Physics*, 3rd ed. (Pergamon, New York, 1980), Part 1, p. 345.
[23] J. W. Loram *et al.*, Philos. Mag. B **65**, 1405 (1992).
[24] A. S. Alexandrov, A. M. Bratkovsky, and N. F. Mott, Phys. Rev. Lett. **72**, 1734 (1994).
[25] A. S. Alexandrov, Phys. Rev. B **48**, 10 571 (1993).
[26] M. S. Osofsky *et al.*, Phys. Rev. Lett. **72**, 3292 (1994).
[27] N. F. Mott, *Conduction in Non-Crystalline Materials* (Clarendon, Oxford, 1993), p. 131.